ELSEVIER

Journal of Organometallic Chemistry 501 (1995) 219–234

Journal of Organometallic Chemistry

The influence of electronic and steric effects and the importance of polymerization conditions in the ethylene polymerization with zirconocene/MAO catalysts ☆

Christoph Janiak [a,*], Uwe Versteeg [a], Katharina C.H. Lange [a], Roman Weimann [a], Ekkehardt Hahn [b]

[a] *Institut für Anorganische und Analytische Chemie, Technische Universität Berlin, Straße des 17. Juni 135, D-10623 Berlin, Germany*
[b] *Institut für Anorganische und Analytische Chemie, Freie Universität Berlin, Fabeckstr. 34-36, D-14195 Berlin, Germany*

Received 20 April 1995

Abstract

A series of $Cp'(C_5H_5)ZrCl_2$ and Cp'_2ZrCl_2 precatalysts ($Cp' = C_5Me_4H$, C_4Me_4P, C_5Me_5) together with $(C_5H_5)_2ZrCl_2$ has been investigated in terms of steric and electronic variations and their catalytic activities in combination with methylalumoxane (MAO) towards the polymerization of ethylene are compared. The changes in the steric environment were evaluated on the basis of the structural data available and supplemented by theoretical structural studies on the semiempirical (ZINDO, EHMO) and density functional (DF) level. The X-ray structures of $(C_5Me_4H)_2ZrCl_2$ (**3**) and $(C_4Me_4P)(C_5H_5)ZrCl_2$ (**4**) have been determined (**3**: orthorhombic, *Cmcm*, $a = 6.714(4)$, $b = 17.275(4)$, $c = 15.643(5)$ Å, $Z = 4$; **4**: monoclinic, $P2_1/c$, $a = 8.8791(5)$, $b = 7.8051(8)$, $c = 20.9215(10)$ Å $\beta = 94.422(4)°$, $Z = 4$. ^{91}Zr NMR data for the above series has been measured and is correlated to changes in the HOMO–LUMO gap available from electronic structure calculations. Under mostly homogeneous polymerization conditions, at very low zirconium concentrations the order of the catalytic activity found for ethylene polymerizations is $(C_5H_5)_2ZrCl_2 > (C_5Me_4H)(C_5H_5)ZrCl_2 > (C_5Me_5)(C_5H_5)ZrCl_2 > (C_4Me_4P)(C_5H_5)ZrCl_2 > (C_5Me_4H)_2ZrCl_2 >> (C_5Me_5)_2ZrCl_2 > (C_4Me_4P)_2ZrCl_2$, which for the most part is inversely proportional to the steric demand of the ring ligands in the metallocene precatalysts except for the phospholyl systems. The lower activities of the phospholyl vs. the tetra- and penta-methylcyclopentadienyl compounds might imply an electronic effect such that the electron withdrawing phosphorus substituent decreases the activity, although further studies are needed to clarify this situation. Emphasis is placed on the control of the polymerization conditions and evaluation of the time-activity profiles. At higher zirconium concentrations an increased precipitation of polyethylene takes place during the course of polymerization and results in a transfer to the heterogeneous phase with a diffusion controlled reaction rate thereby invalidating any activity-comparing studies.

Keywords: Zirconocenes; Metallocene/methylalumoxane catalysts; Catalysis, Ziegler–Natta; Ethylene polymerization; Structure–reactivity correlation; Crystal structure

1. Introduction

Homogeneous, single-site metallocene-methylalumoxane (MAO) catalysts are of high academic and industrial interest as a new generation of Ziegler–Natta catalysts [1–5]. The elucidation of ligand effects has been a central piece of work in zirconocene-MAO catalyzed polymerizations of α-olefins as the catalytic activity and the polymer parameters such as molar mass and molar mass distribution can be tailored through a rational ligand design at the transition metal center. Most investigations into ligand effects in such polymerizations have focused on the influence of the steric environment [1,3,6,7] and comparatively few have addressed the question how electronic changes in a ligand affect the metal center and its catalytic properties [8–11]. Electronic together with steric effects have at times been invoked to explain the influence of different cyclopentadienyl ligand substituents, e.g. by Ewen et al.

☆ Dedicated to Prof. Dr. Herbert Schumann on the occasion of his 60th birthday with gratitude.

* Corresponding author.

SSDI 0022-328X(95)05647-5

[12], Chien and Razavi [13] and Mise et al. [14]. No definitive proof for an electronic effect could be given in these articles, however, since the complexes simultaneously differed in their steric hindrance.

To single out the steric from the electronic effects, Piccolrovazzi et al. employed unbridged indenyl ligands carrying a hydrogen, methyl, methoxy or fluorine ligand in the 4- and 7-position (on the annelated six-membered ring) [8]. A similar approach was taken by Lee et al. who used bridged and unbridged indenyl ligands on a zirconium center which were similarly substituted at the 4- and 7- or 5- and 6-positions [9]. Substituents on the C_6 fragment of these bis(indenyl)zirconium complexes were assumed not to interfere sterically with the incoming monomer, the growing polymer chain or with the insertion reaction at the transition metal center. As a result it was proposed that electron withdrawing groups led to a decrease in catalytic activity and polymer molar mass in the polymerization of ethylene and propylene, while the effect of electron donors was less clear [9]. Recent results with bis(benz[e]indene)- [4] and bis(4-arylindenyl)-zirconium complexes [5] demonstrated, however, a marked steric influence of an aromatic ring annelated or bonded in the 4-position to the C_6 moiety of the indenyl system. Furthermore, the polymerization conditions used in these comparative studies, namely low monomer pressures such as 0.28 or 0.75 bar [8,9] shed doubt on the validity of the results obtained. At ethylene atmospheric pressure of 1 bar or below, diffusion from the gas into the liquid phase becomes the rate-limiting step. Then, the difference in activity rather reflects a difference in activation equilibria and consequently a difference in the concentration of the active species [2,15].

In more profound investigations Möhring and Coville recently reported a quantification of steric and electronic parameters by the use of cone angles and Hammett functions in the ethylene polymerization with $(CpR)_2ZrCl_2$-ethylalumoxane catalysts [10]. Cone angles, NMR-spectroscopic and structural parameters were also used by Möhring et al. to separate the steric and electronic cyclopentadienyl substituent effects of $(C_5H_4R)_2TiCl_2$ and $(C_5H_5)(C_5H_4R)TiCl_2$ catalysts with $Et_3Al_2Cl_3$ as an activator in the polymerization of ethylene [11]. We also note attempts to separate the electronic and steric ligand effects in other areas of catalysis [16].

In accordance with the experimental studies a large number of theoretical calculations have focused on the influence of the steric environment at the metal center [17] and other features such as agostic interactions of the polymer chain with the 14-valence electron zirconium ion [18]. However, we are only aware of one theoretical investigation dealing with electronic effects in alkene polymerizations. There, an attempt was made to substantiate the electronic effects deduced with the aforementioned substituted bis(indenyl)zirconium complexes by AM1 calculations on the free ligands [19].

In this paper we analyze the electronic and steric changes brought upon the metal center in zirconocene dichloride by hydrogen → methyl and CH → P ring substitution with the help of comparative X-ray crystallography, ^{91}Zr NMR spectroscopy and theoretical studies. In order to distinguish between the electronic and steric effects of the ancillary ring ligands on the structure and properties of zirconocenes we compare here a series of compounds which have ligands of similar size, but with different electron-donating abilities, namely tetramethyl- and pentamethyl-cyclopentadienyl vs. tetramethylphospholyl. We investigate how the varying ring substituents and electronic properties affect the catalytic behavior of Cp_2ZrCl_2/MAO for the ethylene polymerization reaction ($Cp = C_5H_5$ and substituted cyclopentadienyl).

2. Results and discussion

2.1. X-Ray structures of $(C_5Me_4H)_2ZrCl_2$ (3) and $(C_4Me_4P)(C_5H_5)ZrCl_2$ (4)

For an assessment of the possible correlation between structure and ^{91}Zr NMR parameters or between structure and catalytic activity, it proved necessary to have as many structural parameters available as possible. In our series of permethylated cyclopentadienyl and phospholyl compounds only the structures of pentamethylzirconocene dichloride, $(C_5Me_5)(C_5H_5)ZrCl_2$ (**6**) [20], and bis(tetramethylphospholyl)zirconium dichloride, $(C_4Me_4P)_2ZrCl_2$ (**5**) [21], were known. With suitable crystals available we therefore determined the X-ray structures of the octamethyl- and the (tetramethyl-phospholyl)(cyclopentadienyl)zirconium derivative **3** and **4**, respectively.

Fig. 1 shows the molecular structure of **3** together with a stereoscopic cell plot. The structure of **4** together with its packing diagram is illustrated in Fig. 2. In both structures the least substituted ring position (C–H or the phosphorus atom) is oriented more in the direction of the intersecting line between the two ring planes to allow for a positioning of the methyl groups towards the maximum opening. In **3** the fully eclipsed arrangement of both tetramethylcyclopentadienyl rings is crystallographically enforced as the zirconium center sits on a special position and the molecule is cut by two mirror planes and only half of a cyclopentadienyl ligand per molecule is symmetry independent (cf. the atomic numbering in Fig. 1). We note that this eclipsed conformation is probably not a very pronounced local minimum with respect to ring rotation. Local minima are calculated at about 30°, 105° and 165° when one ring is rotated around the Zr–ring bond starting at the H,

eclipsed conformation observed in **3**. The population of a higher lying state might be due to the crystallization conditions employed here, such as crystal growth from the gas phase via sublimation. A staggered conformation with the phosphorus atom rotated out of the way of a C–H bond of the opposing cyclopentadienyl ligand is observed in **4** (cf. Fig. 2).

Table 1 compiles the structural data of permethylated zirconocenes and of zirconocene dichloride [23,24] for comparison. Bond distances and angles in **3** and **4** are very similar to those observed in the other structurally characterized permethylated cyclopentadienyl or phospholyl derivatives $(C_5Me_5)(C_5H_5)ZrCl_2$ (**6**) or $(C_4Me_4P)_2ZrCl_2$ (**5**). Generally, a slight increase in bond length towards the more highly substituted ligand in the mixed bent-sandwich compounds **4** and **6** can be noted. This does not necessarily imply a weaker bond, though. Quite to the contrary, mass spectrometrical investigations seem to suggest that the C_5H_5 ring is more weakly bound and more easily lost, at least in the mixed complexes **2** and **6** where the $[C_5H_5ZrCl_2]^+$ fragment is of significantly lower intensity compared to

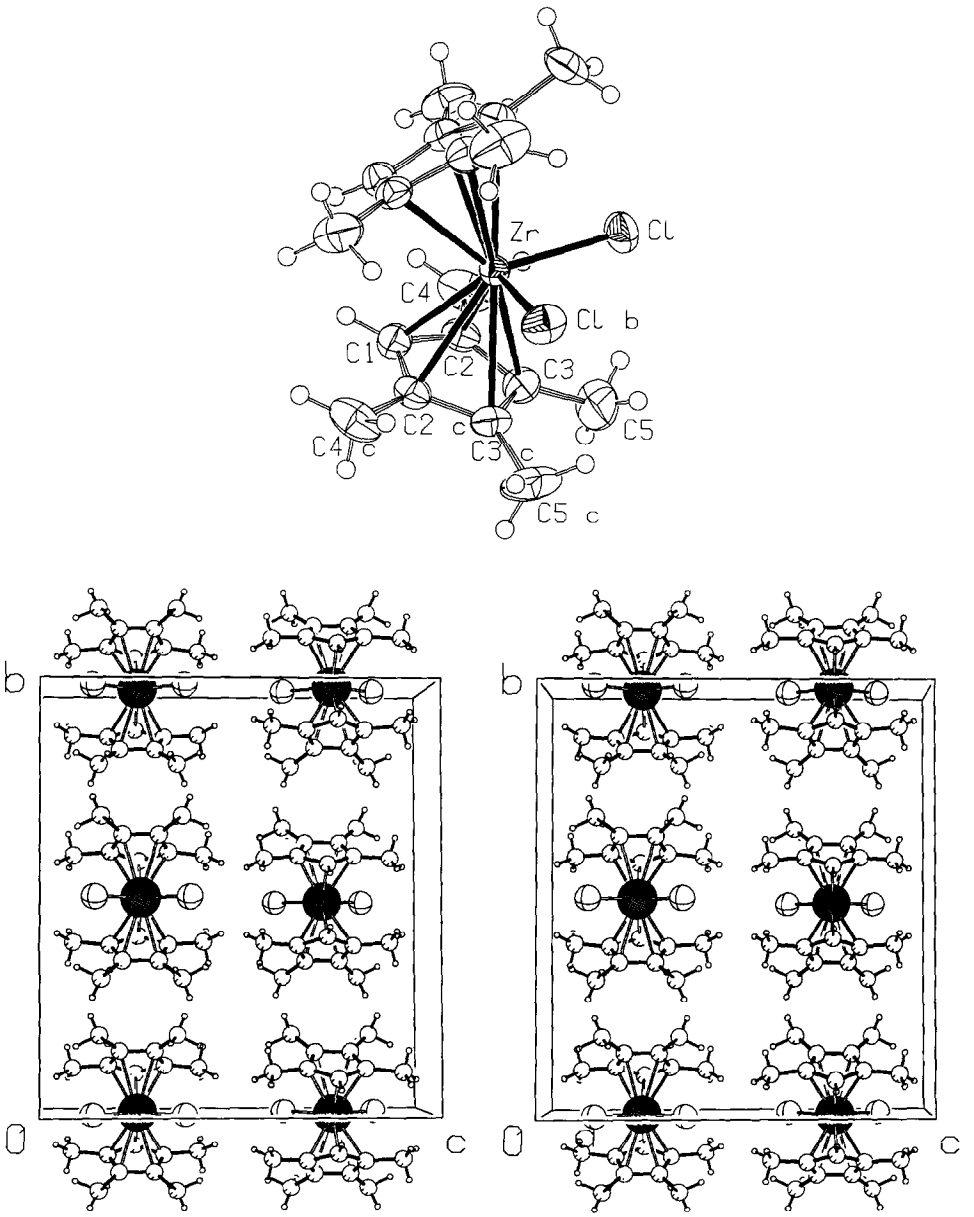

Fig. 1. Molecular structure of $(C_5Me_4H)_2ZrCl_2$ (**3**) with the atomic numbering scheme and stereoscopic cell plot (PLATON-TME, 50% probability ellipsoids, and PLUTON plot, respectively [22]). Selected distances [Å]: Zr-Cl = 2.435(2), Zr–C1 = 2.471(8), Zr–C2 = 2.508(5), Zr–C3 = 2.589(5). Further distances and angles are listed in Table 1.

$[C_4Me_4HZrCl_2]^+$ and especially to $[C_5Me_5ZrCl_2]^+$. This interpretation is presented tentatively, however, since the lower intensity of the $[C_5H_5ZrCl_2]^+$ fragment could also be due to a faster subsequent fragmentation of a less stabilized ion.

There is a gradual increase in the bending angle at the zirconium center with an increase in the steric demand of the ring ligands from 129° in $(C_5H_5)_2ZrCl_2$ towards 135° in $(C_4Me_4P)_2ZrCl_2$ (**5**). At the same time the Zr–Cl distances and the Cl–Zr–Cl angle remain rather invariant at 2.44 Å and 97° to 98°, respectively, except for **5** where an angle of 94.9° was reported [21]. This is in agreement with a structural comparison in symmetrically substituted titanocenes where also no correlation between the ring–Ti–ring and Cl–Ti–Cl angle was observed [11]. For an estimate on some of the structural parameters in $(C_5Me_4H)(C_5H_5)ZrCl_2$ (**2**) and $(C_5Me_5)_2ZrCl_2$ (**7**) see Figs. 3 and 4 and the accompanying text.

2.2. Theoretical calculations and steric effects

Theoretical calculations at varying levels of sophistication have been performed to see how the distances

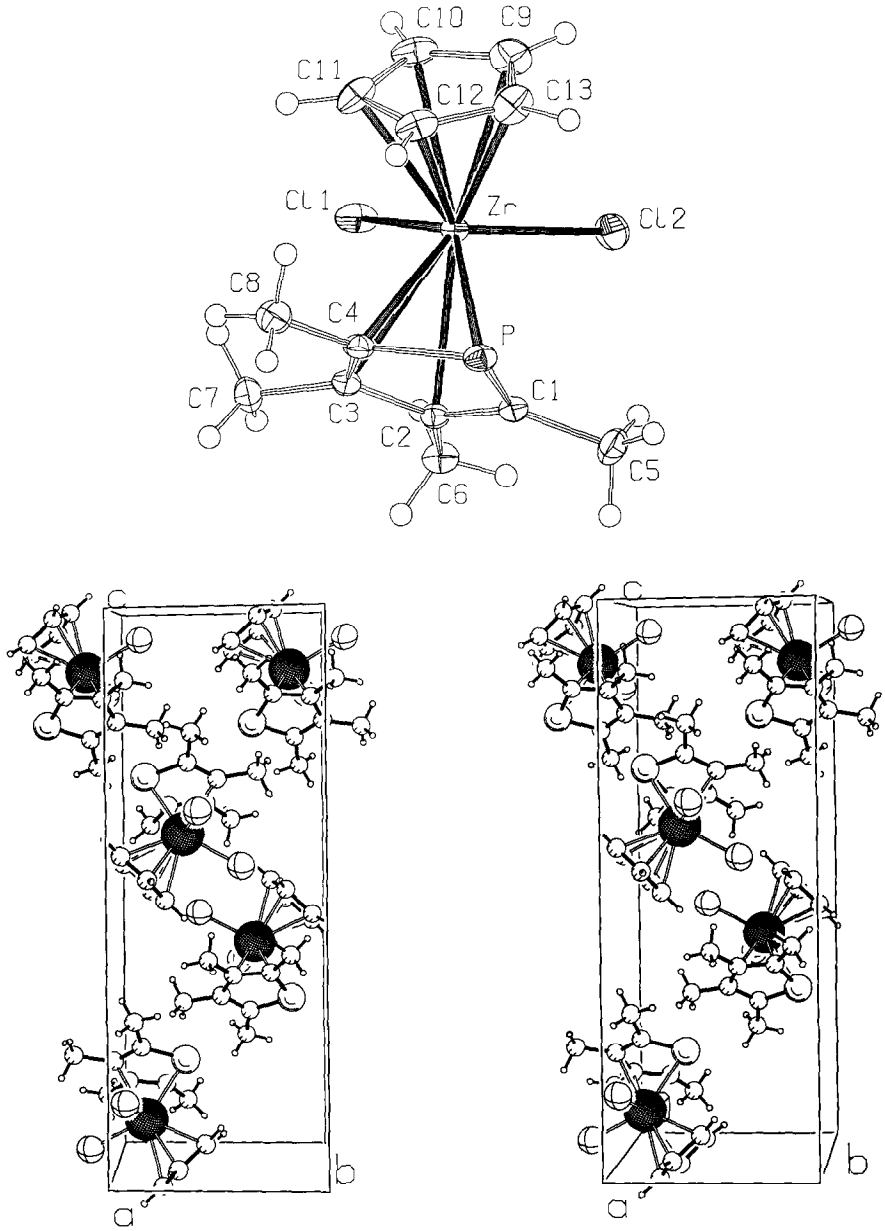

Fig. 2. Molecular structure of $(C_4Me_4P)(C_5H_5)ZrCl_2$ (**4**) (PLATON TME, 50% probability ellipsoids) and stereoscopic packing diagram (PLUTON [22]). Selected distances (Å): Zr–Cl1 = 2.4536(5), Zr–Cl2 = 2.4268(5), Zr–P = 2.7173(5), Zr–C4 = 2.557(2), Zr–C9 = 2.527(2), Zr–C10 2.520(2), Zr–C11 = 2.485(2), Zr–C12 = 2.500(2), Zr–C13 = 2.496(2), P–C1 = 1.766(2), P–C4 = 1.777(2). More distances and angles are given in Table 1.

and angles in structurally known zirconocenes can be reproduced and therefore to estimate the parameters of related analogs. Furthermore, it was hoped to follow the electronic effects exerted on the zirconium center by H → Me and CH → P substitution. Subsequently, these theoretical studies on the steric and electronic trends in our zirconocene series should provide a handle with which to separate the steric and electronic ligand effects for the interpretation of the polymerization activities. As the calculations are carried out on isolated gas-phase molecules, these comparative studies should also serve to estimate to what extent packing effects may influence the structural parameters.

Figs. 3 and 4 illustrate at the case of the zirconium–carbon distances and the centroid–Zr–centroid angle how bond lengths and angles or at least a trend in variation can be reproduced by ZINDO/1 and density functional (DF) calculations. The essentially constant character of the Zr–C distances is represented by both the ZINDO/1 and DF methods, with the latter also giving excellent agreement with the absolute average bond distances as well as with the Zr–C bond length alteration (minimum and maximum Zr–C distance) in the Zr–ring bonding. The same can be said for the Zr–Cl contacts (not shown here). However, the small (albeit possibly significant) changes in the centroid–Zr–centroid angle are at first sight apparently more difficult to reproduce theoretically. Neither of the two methods employed is found to give very good agreement here. The DF results, which lie closer to the experimetal value, still deviate from −2.4° to +2.3°, the ZINDO/1 values even more so, but the latter method appears sometimes to be better suited in predicting the trend observed. We would, however, ascribe this experimental/theoretical discrepancy not so much to a deficiency in the method, as to evidence of packing effects in the solid state structure vs. the minimized gas phase structure. This assertion would have to be tested by crystal packing calculations, of course, for which the methods used here are not well suited. Such packing calculations for a related bridged titanocene were performed by Doman et al. using a molecular mechanics force field method and the results supported the notion that crystal packing forces can have a significant effect on angular parameters [25]. For the yet unknown structures of **2** and **7** we would predict no change in distances and a centroid–Zr–centroid angle of about 131° for **2** and of about 133° for **7** (cf. Fig. 2).

A change in angular parameters was sometimes emphasized in a correlation with the polymerization activities [11] as well as in the interpretation of the ^{91}Zr NMR chemical shifts [26]. To judge the depth of the potential well for the ring–Zr–ring bending mode and, hence, the flexibility or ease of distortion of the angles around the metal, we resorted to extended-Hückel molecular orbital calculations as the ZINDO- and DF-containing programs did not allow for a controlled variation in the ring–Zr–ring angle mostly due to the lack of a dummy atom topology [25]. The energy variation upon ring bending is illustrated in Fig. 5 and shows a shallow minimum only for the unsubstituted zirconocene dichloride. The symmetrical permethylated zirconocene derivatives on

Table 1
Selected bond distances and angles for zirconocene dichloride and permethylated cyclopentadienyl- and phospholylzirconium dichlorides as determined by single-crystal X-ray structural investigations

Compound	Zr–C [a] (Å)	Zr–cnt [b,c] (Å)	Zr–Cl [d] (Å)	cnt–Zr–cnt [b,c] (°)	∠(Cp1, Cp2) [e] (°)	Cl–Zr–Cl (°)	Ref.
1 $(C_5H_5)_2ZrCl_2$	2.494(19)	2.194(9)	2.441(5)	129.1(3)	54(1)	97.1(2)	[23]
3 $(C_5Me_4H_2)ZrCl_2$	2.531(46)	2.226(3)	2.434(3)	133.1(1)	53.7(4)	97.61(9)	this work
4 $(C_4Me_4P)(C_5H_5)ZrCl_2$			2.440(1)	132.34(3)	51.1(1)	97.58(2)	this work
C_4Me_4P-ring [f]	2.633(53)	2.277(1)					
C_5H_5-ring [f]	2.506(16)	2.201(1)					
5 $(C_4Me_4P)_2ZrCl_2$	2.633(57)	2.284(1)	2.436(1)	135.38(4)	47.9(1)	94.90(3)	[21]
6 $(C_5Me_5)(C_5H_5)ZrCl_2$			2.442(1)	130.01(7)	53.4(2)	97.78(3)	[20]
C_5Me_5-ring [f]	2.524(14)	2.219(2)					
C_5H_5-ring [f]	2.507(31)	2.209(2)					

[a] Average distance with statistical variance in parentheses.
[b] cnt = ring centroid of the five-membered cyclopentadienyl or phospholyl ring.
[c] The ring slippage, i.e. the distance between the ring centroid and the normal to the zirconium atom is rather small, at the most 0.13 Å for **3** and 0.10 Å for **4**. Hence, the Zr-centroid distance and the ring normal Zr are essentially equal (differing by less than 0.01 Å). A larger difference is calculated between the centroid-Zr-centroid angle and the angle made by the two normals from the Zr center to the ring planes (2.6° for **1**, 6.8° for **3**, 2.4° for **4**, 3.3° for **5**, and 3.4° for **6**). The angle between the two projections, normals of the zirconium atom onto the ring planes calculates according to "180°-∠(Cp1, Cp2)".
[d] Average distance and standard deviation.
[e] Angle made by the two ring planes at their intersection, interplanar angle.
[f] For the fixed bent-sandwich complexes the Zr–C and Zr-cnt distances are listed separately for both rings.

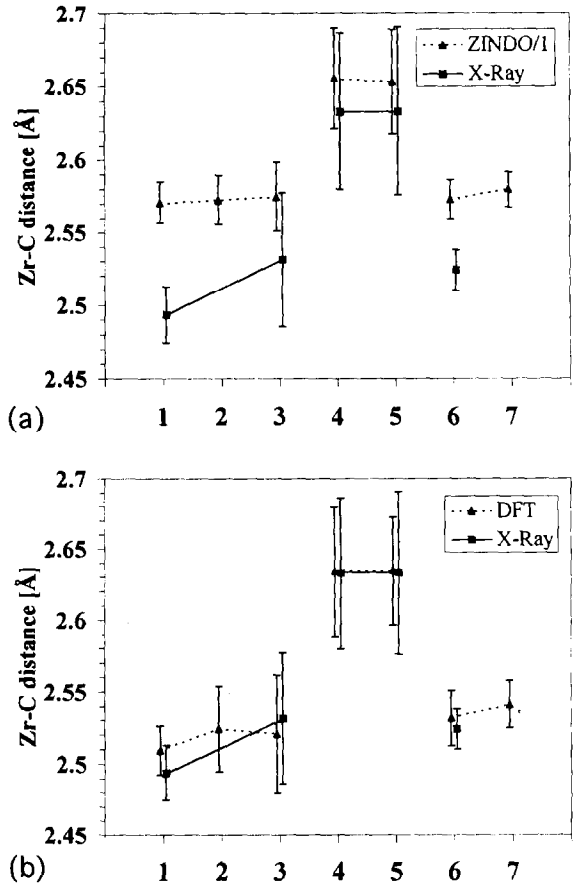

Fig. 3. ZINDO/1 (a) and DF (b) calculations on the Zr–C distances in **1-7** and comparison to experimental values from single-crystal X-ray data, where available (for references, see Table 1). The error bars indicate the variance observed or calculated in the Zr–C bond lengths. For a better comparison of the experimental and theoretical results, the symbols marking the average value together with the variance are not plotted on top of each other. The connecting lines are meant as visual aids in the comparison of the respective mixed and symmetrical complex.

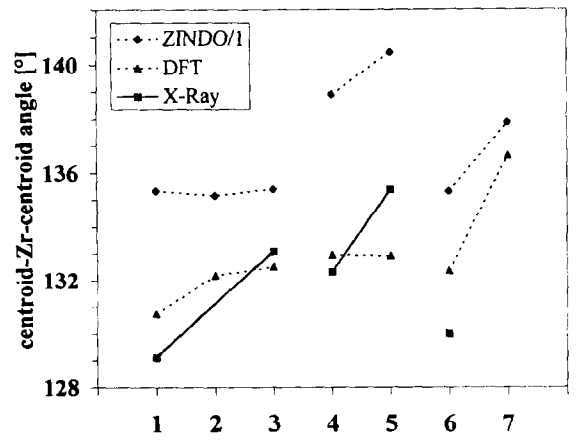

Fig. 4. ZINDO/1 and DF calculations on the centroid-Zr-centroid angle in **1–7** and comparison to experimental values from single-crystal X-ray data, where available (for references see Table 1). The connecting lines are meant as visual aids in the comparison of the respective mixed and symmetrical complex.

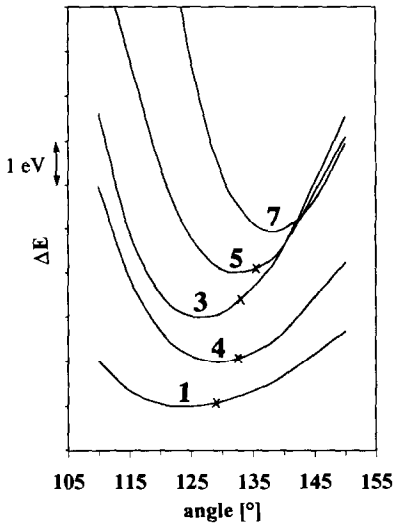

Fig. 5. Potential wells for the (ring centroid)–Zr–(ring centroid) bending in the zirconocene series **1–7** based on EHMO calculations. For clarity only one of the similar curves is shown for the mixed sandwich complexes (**4**). Note the narrowing of the wells when going from (unsubstituted) zirconocene dichloride (**1**) over the mixed tetramethylphospholyl sandwich (**4**) to the octamethyl- (**3**), bis(tetramethylphospholyl)- (**5**) and decamethylzirconocene derivatives (**7**). The respective experimental minimum position from X-ray structural studies is indicated by an x.

the other hand have a rather well developed minimum, which narrows from octamethyl- over bis(tetramethylphospholyl) to decamethylzirconocene (**3** → **5** → **7**), thus, there is less conformational flexibility in adjusting the gap aperture (Fig. 6) [27]. A potential well of intermediate depth is calculated for the mixed bent-sandwich complexes.

The electronic results from the DF calculation will be discussed together with the ^{91}Zr NMR results in the next section.

2.3. ^{91}Zr NMR studies and electronic effects

The transfer of electronic effects from various, mainly alkyl substituents on the cyclopentadienyl rings to the

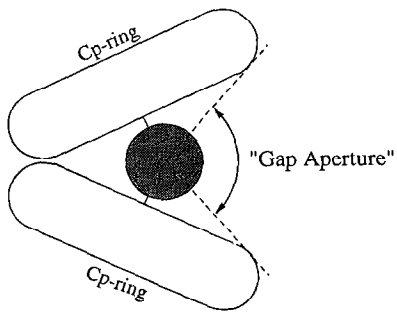

Fig. 6. Schematic representation of the gap aperture of a bei metallocene based on the van-der-Waals surface of the ring ligand The gap aperture means the maximum opening angle, taking int account ring substituents which do not have to lie in the paper plar [27].

central metal in zirconocene complexes is already well substantiated by photoelecton spectroscopy (PES) studies and ^{91}Zr NMR. The seminal work of Gassman et al. demonstrated with ESCA studies on the series zirconocene, penta- and decamethylzirconocene dichloride a sequential lowering of the binding energies of the inner shell Zr 3d electrons [28]. In addition, XPS studies revealed that the relative electronic difference between the three precatalysts is essentially retained upon activation with MAO [29]. ^{91}Zr NMR spectroscopical investigations on ring-substituted zirconocene dichlorides also showed an electronic change at the metal as the chemical shift, $\delta(^{91}Zr)$, is inversely proportional to the average electron excitation energy which in turn relates to the HOMO–LUMO gap [26,30].

It was suggested, however, especially in connection with the NMR chemical shifts, that these electronic changes exerted on the zirconium center may not be due to a direct inductive effect from the ring substituent but that they are a consequence of the inevitable angle variations initiated by the steric differences [26]. In an MO-theoretical study on the structure and chemistry of the bent bis(cyclopentadienyl)metal fragment, Lauher and Hoffmann showed how the bending of the cyclopentadienyl ligands affects the metal frontier orbitals [31].

Photoelectron spectroscopy investigations on permethylated zirconocenes [28,29] and ferrocenes [32,33] indicate an electron donating effect of the methyl substituents corresponding to an additive decrease in ionization potential of about 0.08 eV per methyl group. Phosphorus in a phospolyl ligand increases the binding energies of the valence electrons, however, by 0.2 eV in the case of 1,1'-diphosphaferrocene [34], thus, exerting an electron withdrawal effect.

For a handle on the electronic variability in the zirconocene series **1–7** we have measured the ^{91}Zr NMR spectra of the complexes and performed electronic structure calculations. The chemical shift data is listed in Table 2. Also included in Table 2 is the difference in HOMO–LUMO energy (the HOMO–LUMO gap) and the charges on the zirconium center from DF-theoretical calculations. With respect to the calculated charges we find it difficult to fully reproduce the expected trend in electron-donating effects when going from the mixed to the symmetrical tetra- and penta-methylcyclopentadienyl complexes. There is also no additive trend on the electron-withdrawing part of the phospholyl-containing species. Unfortunately, the zirconium chemical shifts do not correlate directly with the charge density at the metal, instead a reciprocal electron excitation energy dependence is observed. Other factors being similar, this energy difference can be correlated to the HOMO–LUMO gap in MO-diagrams [30]. When the shifts are scaled to $(C_5H_5)_2ZrCl_2$ the additive nature of ring substitution becomes more obvious. Considering the experimental errors because of the frequency width of the often broader signals, the respective chemical shift of the symmetrical zircononcene is about twice that of the related mixed bent-sandwich. Furthermore, the tetra-, octa- and the deca-methylzirconocenes can be matched to a chemical shift of about 20 ppm per methyl group. Thus, we are confident that the difference in chemical shifts here is due to the electronic changes induced by the ring modifications and is only to a minor extent, if at all, a consequence of the ring–Zr–ring angle variation [26]. (An EHMO-calculation also indicated no significant change in the HOMO–LUMO gap in a ring–Zr–ring angle range between 120° and 140°.) The reciprocal correlation of

Table 2
^{91}Zr-NMR data, calculated HOMO–LUMO energy differences and atomic charges on zirconium for the zirconocene complexes **1–7**

Compound	$\delta(^{91}Zr)$ [a] (ppm)	$\omega_{1/2}$ [b] (Hz)	$\delta(^{91}Zr)$ [c] (ppm)	ΔE [d] (eV)	Zirconium charges [e]	Ref. [f]
1 $(C_5H_5)_2ZrCl_2$	−113	260	0	3.130	0.406	[30]
2 $(C_5Me_4H)(C_5H_5)_2ZrCl_2$	−22	500	81	2.995	0.432	
3 $(C_5Me_4H)_2ZrCl_2$	54	810	167	2.952	0.393	
4 $(C_4Me_4P)(C_5H_5)ZrCl_2$	29	1760	142	3.050	0.395	
5 $(C_4Me_4P)_2ZrCl_2$	170	3030	283	2.906	0.300	
6 $(C_5Me_5)(C_5H_5)ZrCl_2$	10	340	123	2.985	0.450	
7 $(C_5Me_5)_2ZrCl_2$	87	140	200	2.840	0.449	[30]

[a] Chemical shift from $(C_5H_5)_2ZrBr_2$ with $\delta = 0$ ppm.
[b] Frequency width at half-height maximum.
[c] Chemical shift based on $(C_5H_5)_2ZrCl_2$.
[d] HOMO–LUMO gap from a density functional calculation.
[e] Mulliken net atomic charges from a DF calculation.
[f] References to literature data available for comparison.

the HOMO–LUMO gap with chemical shifts leads to a smaller orbital energy difference with increasing methyl substitution for the permethylated cyclopentadienyl systems, although the calculated gap variation appears quite small. A smaller HOMO–LUMO difference can be due to an energy increase of the filled level, a decrease of the empty level, or both. An increase of the filled levels would be expected for electron-donating (methyl-) substituents.

The direction of the chemical shifts of the phospholyl compounds with respect to each other and to the permethylated cyclopentadienyl systems is, however, not satisfactorily explained along these lines. For the bisphospholyl system **5** we would, for example, predict a higher electron withdrawing effect, and hence expect a larger excitation energy (or HOMO–LUMO gap) compared to **3** and **4**.

This leads us to conclude that ^{91}Zr NMR spectroscopy is not necessarily an optimal method in studying electronic effects except maybe for a very closely related series of compounds. It should not be overlooked that the reciprocal ΔE (HOMO–LUMO gap) dependence is a first, crude approximation only and that more parameters can determine the chemical shift [30].

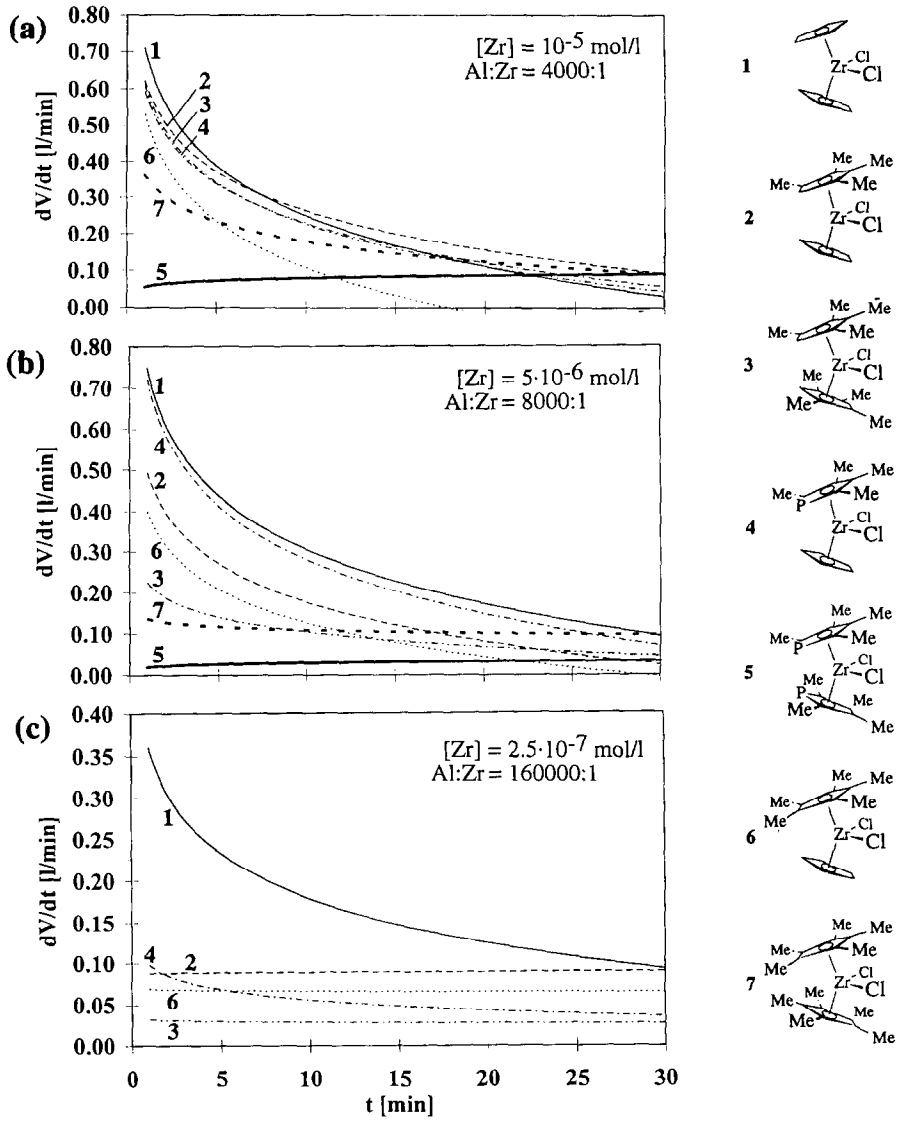

Fig. 7. Activity profiles in the ethylene polymerization for the different zirconocene dichlorides **1–7** activated with MAO at a zirconium concentration/molar Al:Zr ratio of (a) 10^{-5} mol l^{-1}/4000:1, (b) 5×10^{-6} mol l^{-1}/8000:1 and (c) 2.5×10^{-7} mol l^{-1}/160000:1. For further experimental conditions see Table 3. In (c) the very low active complexes **5** and **7** are not included. For a better structure–activity correlation the complexes are sketched at the right hand side.

Table 3
Ethylene polymerization activity [a] with zirconocene/MAO as a function of Zr concentration and molar Al:Zr ratio [b]

Compound	Conditions [c]		
	A	B	C
1 $(C_5H_5)_2ZrCl_2$	37	100	756
2 $(C_5Me_4H)(C_5H_5)ZrCl_2$	30	51	462
3 $(C_5Me_4H)_2ZrCl_2$	30	27	165
4 $(C_4Me_4P)(C_5H_5)ZrCl_2$	37	76	262
5 $(C_4Me_4P)_2ZrCl_2$	11	15	14
6 $(C_5Me_5)(C_5H_5)ZrCl_2$	30	34	373
7 $(C_5Me_5)_2ZrCl_2$	19	27	35

[a] Activity in kg PE/g Zr h bar.
[b] T = 70°C, ethylene pressure 5 bar, 300 ml toluene, polymerization time 30 min.
[c] A $[Zr] = 10^{-5}$ mol l^{-1}, Al:Zr = 4000:1; B $[Zr] = 5 \times 10^{-6}$ mol l^{-1}, Al:Zr = 8000:1, C $[Zr] = 2.5 \times 10^{-7}$ mol l^{-1} Al:Zr = 160000:1.

2.4. Polymerization studies

The size of the tetramethylphospholyl ligand, defined by its cone angle [1], lies between the size of the tetramethyl- and pentamethylcyclopentadienyl system, yet the C_4Me_4P group is less donating than C_5Me_4H albeit still more so than C_5H_5 (see above, Section 2.3). It was the purpose of the polymerization experiments to check whether these electronic effects would manifest itself in the catalytic insertion reaction. We intentionally employed only ethylene as a monomer in our comparative studies, as with propene the stereospecifity of the catalyst also strongly effects the activity and is thereby able to overcompensate electronic and steric influences [6,38,39].

Furthermore, polymerization reactions of ethylene with **1–7** and methylalumoxane (MAO) as a cocatalyst were carried out with different zirconocene concentrations and different Al:Zr ratios to single out the role of polymerization conditions. Table 3 compares the activities at three different zirconium concentrations. At the same time, the Al:Zr ratio was also increased to offset the higher degree of dissociation upon dilution of the catalytically active complex in the complexation equilibrium (eqn. (1)) [2].

$$Cp_2ZrX_2 + n\text{MAO} \rightleftharpoons \{(Cp_2ZrR)^+(\text{MAO})_n^-\}^{\ddagger} \quad (1)$$

At the highest zirconium concentration employed here in the polymerization experiments (10^{-5} mol l^{-1}) the activities are rather similar, only the bulky complexes **5** and **7** already show significantly lower values. When comparing the activities for a given catalyst at different concentrations and cocatalyst ratios a drastic increase is generally seen towards lower concentration, except again for **5** and **7**. The magnitude of increase strongly depends on the catalytic complex, however, and the systems already differentiate considerably in their activity when lowering the Zr-concentration to 5×10^{-6} mol l^{-1} with an Al:Zr-ratio of 8000:1.

The similarity in activities of **1** and **4**, or **2**, **3** and **6** at the high-concentration regime is due to the fact that polyethylene precipitates rapidly under these conditions, all the faster the more active the catalyst. The polymerization is truly homogeneous only in the very beginning. Having the active complex embedded in a polymer matrix represents a transfer to a heterogeneous phase, i.e. a heterogeneous active complex form, and leads to a diffusion-controlled polymerization. The reaction rate is then controlled by the rate of the diffusion process of the monomer through the polymer matrix to the enclosed active center [40–42] and can no longer be compared in terms of electronic or steric effects. Fig. 7(a) illustrates this fact by showing the difference in ethylene uptake over time for an Al:Zr ratio of 4000:1. The differential ethylene consumption (dV/dt) is a direct measure of the activity at the time t. One realizes that the time-activity profiles show a steady decline (except for **5**) and are essentially the same within experimental error after about 5 min for **1–4** and after ca. 15 min even for **7**. The equal activity after this time is due to the diffusion controlled reaction because of polymer precipitation. The differences in activity given in Table 3 are then due to the activity differences during the first minutes in a still more homogeneous reaction mixture. One could then argue that the initial rate in the very beginning (first few seconds) of the polymerization should correspond to a characteristic rate for the homogeneous catalyst and reflect the electronic and steric variations. It is, however, difficult to monitor these initial rates [40,42] and especially so in view of the high activities of the methylalumoxane activated zirconocene systems, or to extrapolate the rates to $t = 0$ from the profiles in Fig. 3 with a high enough accuracy because of the very similar rates which have been reached for **1–4** after one minute already.

The activity profiles for the series with the zirconium concentration of 5×10^{-6} mol l^{-1} (Al:Zr ratio 8000:1) in Fig. 7(b) show a greater diversity in the first minutes but they still approach the diffusion controlled rate limit ($dV/dt \leq 0.1$ l min^{-1}) due to polymer precipitation. The increase in activity for a given catalyst with decreasing Zr concentration and increasing Al:Zr ratio can be traced to two origins: (i) to a later precipitation of polymer together with the change to the diffusion-controlled rate limit, such that in the diluted solutions

[1] Cone angles of 188°and 148° were reported for C_5Me_5 and C_5H_5, respectively, when π-bonded to a metal (Rh(III)) with a ring-centroid to metal distance of 1.9 Å [35,36]. The cone angle θ_1 of an n substituted ring $C_5H_{5-n}R_n$ then calculates as $\theta_1 = (5-n)\alpha/5 + n\beta/5$, with α and β being the cone angles for C_5H_5 and C_5R_5, respectively [37]. Hence, a cone angle of 180° is obtained for C_5Me_4H and the cone angle for C_4Me_4P will lie between 180° and 188°.

the homogeneous complex with its higher activity dominates the polymerization profile [2]; (ii) to the known "infinite" increase in activity with the increase of the Al : Zr ratio [43–46].

At a zirconium concentration of 2.5×10^{-7} mol l^{-1} together with an Al : Zr ratio of 160 000 : 1 the integrated turnover for the complexes in this series is decreased further and lies below or around the diffusion rate limit, so that the activity profiles show a constant ethylene consumption (Fig. 7(c)). The lower amount of polyethylene produced in these polymerization experiments assures the existence of a homogeneous phase over an extended time period, the highly active $(C_5H_5)_2$Zr-system being a notable exception. Consequently, other things being equal, the difference in activities should now reflect the searched for difference in steric or electronic characteristics. There is just one uncertainty remaining: this concerns the effect of the dynamic activation equilibria as outlined in eqn. (1). The same Al : Zr ratio can lead to a different equilibrium position, i.e. to a different relative concentration of the active species for the various zirconocenes **1–7**. This difference is, of course, also a consequence of the differences in the steric and electronic requirements of the complexes. Since the full functionality of MAO and most importantly its interaction with or its role in the activated metallocene is not known [47], it is, however, difficult to judge the relative influences. In principle, it is possible that a single active species A* polymerizes faster than a species B*, yet the activation equilibrium of A is such that there is a lower concentration of A*, leading to a lower overall "apparent" polymerization rate [15].

To circumvent this problem of the activation equilibrium one might add enough MAO to shift the equilibrium almost completely to the side of the active complex. We have therefore investigated the activity of $(C_5H_5)_2ZrCl_2$ at various Zr concentrations and feasible Al : Zr ratios (at a constant Al concentration) to see if a limit could be reached. Fig. 8 shows the time-activity profiles normalized to the molar zirconium content for different Zr concentrations and Al : Zr ratios. If the equlibrium position, i.e. the relative concentration of active species, were the same and an acitivation limit were reached one should see the same normalized differential acitvity. This is not the case, however; instead one finds again an increase in activity with increasing cocatalyst-to-catalyst ratio [43–46]. Hence, we cannot say anything on the dynamic activation equilibria and are left with a correlation of the steric and electronic features of the complex to the apparent activity.

The order of this "apparent" catalytic activity found for ethylene polymerizations in our zirconocene series at the homogeneous, low zirconium concentration end is $(C_5H_5)_2ZrCl_2$ **(1)** > $(C_5Me_4H)(C_5H_5)ZrCl_2$ **(2)** > $(C_5Me_5)(C_5H_5)ZrCl_2$ **(6)** > $(C_4Me_4P)(C_5H_5)ZrCl_2$ **(4)** > $(C_5Me_4H)_2ZrCl_2$ **(3)** > > $(C_5Me_5)_2ZrCl_2$ **(7)** > $(C_4Me_4P)_2ZrCl_2$ **(5)** (cf. Table 3, column C; Fig. 7(c)). For the most part, this ordering with the unsubstituted zirconocene more active than the mixed sandwiches and these again more active than the symmetrically, substituted zirconocenes can be explained on steric grounds. On the molecular level we can invoke here a steric hindering of the methyl substituents together with a decreasing flexibility in adjusting the gap aperture towards the spatial requirements of the incoming monomer and the growing chain. Also, the higher activity of the tetramethyl- over the pentamethyl–cyclopentadienyl

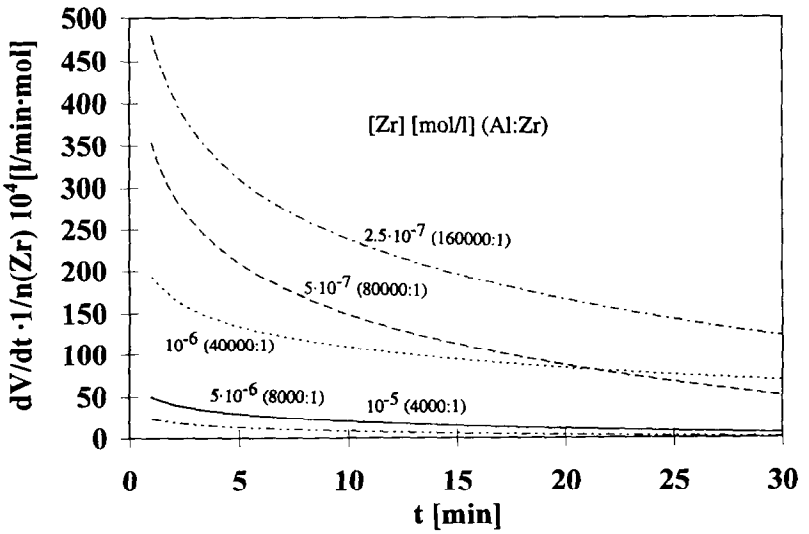

Fig. 8. Activity profiles normalized to moles zirconium in the ethylene polymerization with $(C_5H_5)_2ZrCl_2$/MAO **(1)** at different zirconium concentrations and molar Al : Zr ratios as indicated. The Al concentration remained constant at 4×10^{-2} mol l^{-1}. The activities in the order of decreasing Zr-concentration were as follows: 37, 55, 100, 394, 521 and 756 kg PE/g Zr h bar. Polymerization conditions: $T = 70$°C, 5 bar ethylene, 300 ml toluene, polymerization time 30 min.

derivatives fits into this explanation. The respective lowest activities among the mixed or symmetrical sandwiches for the phospholyl compounds, however, seem to suggest an electronic effect and support the conclusions by Piccolrovazzi et al. [8] and Lee et al. [9] that electron withdrawing groups decrease the activity. We would remain cautious, however, since it is not clear to what extent a functional substituent, such as phosphorus in our case or fluorine or chlorine in the work of Piccolrovazzi or Lee, will interact with a Lewis-acidic aluminum center on the methylalumoxane/trimethylaluminum cocatalyst and thereby change the steric features of the catalytic center (trimethylaluminum is always present to a considerable extent in a MAO solution). Further work on this problem is in progress.

The trend of decreasing activity with increasing steric ligand demand found for our catalytic activities matches the trends observed by Möhring et al. on a $(C_5H_4R)(C_5H_5)TiCl_2/Et_3Al_2Cl_2$ catalyst series [11] and by Kaminsky et al. in a comparative study involving bridged and unbridged zirconocenes [6] as well as pentamethylcyclopentadienyl complexes [43]. In all three studies the highest activity was found for the unsubstituted system. Trends which seem at first conflicting were, however, reported by Chien and Razavi [13], Nekhaeva et al. [48], Möhring and Coville [10] and Tian and Huang [49] who observed an increase of the catalytic activity with increasing size of the substituent. A closer look explains some of these discrepancies, though: Chien and Razavi reported the effect of alkyl substitution on the cyclopentadienyl ring for several compounds and the order of activity was found to be $(C_5MeH_4)_2ZrCl_2 > (C_5EtH_4)_2ZrCl_2 > (C_5NmH_4)_2ZrCl_2$ (Nm = Neomenthyl) > $(C_5H_5)_2ZrCl_2 > (C_5Me_5)(C_5H_5)ZrCl_2 > (C_5Me_5)_2ZrCl_2$ [13]. While a higher activity for small single alkyl substituent was also supported by Tian and Huang, a higher activity for the bulky neomenthyl group over unsubstituted zirconocene appears doubtful, in particular, since no direct comparison under the same catalytic conditions was carried out and the activity data for the other complexes was collected from the sources of other workers, thus involving different Zr concentrations, Al : Zr ratios, temperatures, monomer pressures, not to mention different MAO characteristics, which we feel renders a comparison invalid.

Möhring and Coville also described an increase in activity for $(C_5RH_4)_2ZrCl_2$ with single alkyl substituents and in part with increasing size such that the order of activity was R = t-Bu > $SiMe_3$ > Et > i-Pr > Me = CMe_2Ph > H [10]. Ethylalumoxane was used as a cocatalyst, though, and this was given as a possible reason for these unexpected results. We note here that results by us involving t-butyl substituted zirconocenes, including $(C_5{}^tBuH_4)_2ZrCl_2$ and $(C_5$t-$BuH_4)(C_5H_5)ZrCl_2$, activated by MAO failed to show an increase in ethylene polymerization activity compared to $(C_5H_5)_2ZrCl_2$ [50].

Nekhaeva et al. reported an activity order of $(C_5\{SiMe_3\}H_4)_2ZrCl_2 > (C_5H_5)_2ZrCl_2 > (C_5$t-$BuH_4)_2ZrCl_2$ in ethylene polymerization and suggest an explanation on electronic grounds [48]. Experiments by Tian and Huang at ethylene pressures of 1.5 bar gave a higher activity for $(C_5$n-$PrH_4)_2ZrCl_2$ and $(C_5$n-$BuH_4)_2ZrCl_2$ than for $(C_5H_5)_2ZrCl_2$ [49]. We would like to note, though, that neither of the comparative studies on the single alkyl substituted systems appear to involve determinations of the activities at different polymerization conditions or recording of time-activity profiles.

Finally, we would like to mention the irreversible catalyst deactivation as a further source of different catalyst activities. Kinetic studies on the ethylene and propene polymerization with $(C_5H_5)_2ZrCl_2$/MAO [15,51,52] suggest the existence of a reversible followed by an irreversible deactivation to explain the decay of the polymerization rate as a function of time. We are not aware of any comparative study on how the ligand characteristics of a zirconocene catalyst influence the rate of the irreversible deactivation, but it is sensible to assume different stabilities for different complexes. Hints from the activity profiles of the mixed ligand complexes $(C_5Me_5)(C_5H_5)ZrCl_2$ (**6**) in Fig. 7(a,b) and $(C_4Me_4P)(C_5H_5)ZrCl_2$ (**4**) in Fig. 7(c) where a relatively rapid decay in activity is observed suggest that such irreversible deactivation processes might play a role here under certain conditions. The irreversible deactivation for $(C_5H_5)_2ZrCl_2$/MAO was found to be relatively slow at 60°C [15].

In summary, the data in Table 3 illustrate how polymerization conditions, such as catalyst concentration and cocatalyst-to-catalyst ratio can affect the outcome of otherwise standardized, comparative ethylene polymerizations, because of the phase transfer problem encountered here. In a homogeneous polymerization steric effects play the dominant role in determining the catalytic activity. To investigate this steric/electronic controversy further and to substantiate the above results we will now carry out olefin-oligomerization reactions with propene and 1-hexene as monomers.

3. Conclusions

Comparative X-ray structural studies on the series of permethylated zirconocenes illustrate the extent of bond length and angle variations upon the steric changes. Theoretical geometry optimizations by the density functional and ZINDO/1 methods can be used to predict the geometrical features of related unknown complexes and point out packing effects. Spectrometrical data obtained by ^{91}Zr NMR indicates electronic changes at the zirco-

nium center; it is, however, difficult to interpret these changes in terms of electron donation and withdrawal by the ligand or in terms of different charge densities at the metal. The possibility of electronic effects has been tested by comparative catalytic ethylene polymerizations of the zirconcocene dichloride series with methylalumoxane (MAO) as a cocatalyst. Meaningful results are only obtained under polymerization conditions which allow for a mostly homogeneous reaction system. The phase change upon polyethylene precipitation strongly affects the relative rates in the zirconocene series which can then no longer be compared in terms of steric or electronic effects. The relative rates in the permethylated cyclopentadienyl and phospholyl zirconium series are dominated by steric effects such that any potential electron donating effects by the methyl groups are not seen. Indications on a possible electron withdrawing effect by the ring phosphorus have to be investigated further and cannot yet unequivocally assigned.

4. Experimental details

4.1. Instruments

CHN analysis, Perkin Elmer Series II CHNS/O Analyzer 2400; NMR spectroscopy, Bruker ARX 200 or ARX 400 (^{1}H and ^{13}C chemical shifts are referenced to TMS, ^{31}P to external 85%-H_3PO_4, ^{91}Zr NMR spectra were measured at ambient temperature against Cp_2ZrCl_2 as external reference [dissolved in an 8:1 mixture of CH_2Cl_2/CD_2Cl_2] with $\delta = -113$ ppm from Cp_2ZrBr_2 [30]); mass spectrometry, Varian MAT 311A/AMD (mass spectrometry peaks given refer to the most abundant isotope combination, which contains ^{90}Zr, ^{35}Cl, except when two chlorines are present. In this case, the peak arising from $^{90}Zr^{35}Cl^{37}Cl$ and $^{92}Zr^{35}Cl_2$ is of maximum intensity, as proven by an isotope simulation, but the $^{90}Zr^{35}Cl_2$ peak is cited to match the fragment losses).

4.2. Materials

The known zirconocene dichlorides were prepared according to literature procedures, or slight modifications thereof, as given below. All complexes were purified by sublimation and the purity was checked by melting points, elemental analyses, ^{1}H and ^{13}C NMR spectroscopies and mass spectrometry. The analytical data matched the literature values. Analytical data obtained by us and not previously cited in the literature is given below. $(C_5H_5)_2ZrCl_2$ was purchased from Merck and used as such. Methylalumoxane (MAO) was obtained from Witco (Bergkamen, Germany) as a 10 wt.% toluene solution (4.92 wt.% aluminum, density $\approx$ 0.9 g ml^{-1}, average molecular weight of the MAO oligomers 900–1100 g mol^{-1}). Solvents were dried over sodium metal (toluene and benzene), sodium benzophenone ketyl (pentane and diethyl ether) or potassium metal (hexane and THF) followed by destillation and storage under argon. Ethylene (BASF AG) was polymerization grade and used without further purification. All experiments were carried out under argon with standard Schlenk techniques.

4.3. $(C_4Me_4H)(C_5H_5)ZrCl_2$ (2)

To a mixture of 1.37 g (3.9 mmol) of solid cyclopentadienylzirconium trichloride(dimethoxyethane) [53] and of 0.53 g (4.1 mmol) of solid tetramethylcyclopentadienyllithium were added 25 ml of toluene at −50 °C. After stirring for 20 min at this temperature the reaction mixture was allowed to warm to room temperature within 1 h and the dark brown slurry was heated to reflux for an additional 2 h. After this time the toluene was removed in vacuo and the dark brown residue washed once with 30 ml of hexane followed by continuous extraction with 60 ml of hot hexane over a sinter frit for 19 h. The cold solvent was decanted from the precipitate and the dried grey powder sublimed at 140–150°C/0.5 Torr for 4 d to yield 0.63 g (46%) of fine, pale yellow needles. M.p. 222°C. ^{1}H NMR (200.13 MHz, $CDCl_3$): $\delta = 2.02$ (s, 6H, CH_3C), 2.04 (s, 6H, CH_3C), 5.98 (s, 1H, C–H), 6.36 (s, 5H, C_5H_5). ^{13}C NMR (50.32 MHz, $CDCl_3$): $\delta = 12.01$ (CH_3), 14.20 (CH_3), 111.23 (C–H), 115.29 (C_5H_5), 122.37 (CH_3C-2), 129.82 (CH_3C-3). ^{91}Zr NMR (37.33 MHz, CH_2Cl_2/CD_2Cl_2): $\delta = -22$ ($\omega_{1/2} = 500$ Hz). MS (70 eV, 100°C): $m/e = 346$ (34%, $M^{+\cdot}$), 310 (100, $[M-HCl]^{+\cdot}$), 295 (11, $[M-HCl-CH_3]^+$), 281 (49, $[M-C_5H_5]^+$), 274 (15, $[M-2HCl]^{+\cdot}$), 253 (7, $[M-C_5H_5-C_2H_4]^+$), 245 (22, $[M-C_5H_5-HCl]^+$), 241 (21 $[M-C_5H_5-HCl-2H_2]^+$) [2], 225 (16, $[M-C_5Me_4H]^+$), 199 (7, $[M-C_4Me_4H-C_2H_2]^+$), 190 (7, $[M-C_4Me_4H-Cl]^{+\cdot}$), 121 (9, $[C_5Me_4H]^+$), 105 (26, $[C_5Me_4H-CH_4]^+$). Anal. Found: C, 48.18; H, 5.05%. $C_{14}H_{18}Cl_2Zr$ (348.43); Calc.: C, 48.26; H, 5.21%.

4.4. $(C_4Me_4H)_2ZrCl_2$ (3) [54]

M.p. 211°C. ^{91}Zr NMR (37.33 MHz, CH_2Cl_2/CD_2Cl_2): $\delta = 54$ ($\omega_{1/2} = 810$ Hz). MS (70 eV, 130°C): $m/e = 402$ (62%, $M^{+\cdot}$), 366 (100, $[M-HCl]^{+\cdot}$), 351 (13, $[M-HCl-CH_3]^+$), 281 (68, $[M-C_5Me_4H]^+$), 253 (6, $[M-C_5Me_4H-C_2H_4]^+$), 241 (16, [M–HCl–2H–

[2] A DADI (direct analysis of daughter ions) and a CA (collisional activation) experiment together with an isotope distribution simulation support the formulation of a loss of an HCl and two H_2 molecules from the respective $CpZrCl_2^+$ mother ion Cp = C_5H_5 and substituted C_5 or phospholyl ligands.

$_2]^+)^2$, 122 (12, $[C_5Me_4H + H]^{+\cdot}$), 121 (11, $[C_5Me_4H]^+$), 105 (16, $[C_5Me_4H-CH_4]^+$).

4.5. $(C_4Me_4P)(C_5H_5)ZrCl_2$ (4)

A solution of 0.82 g (5.6 mmol) of tetramethylphospholyllithium [21] in 20 ml of THF was added dropwise over 30 min to a suspension of 2.03 g (5.8 mmol) of cyclopentadienylzirconium trichloride(dimethoxyethane) [53] in 20 ml of THF and cooled to −15°C. The tan-colored reaction mixture was warmed to room temperature and the solvent evaporated in vacuo. The yellow–brown residue was extracted with 40 and 20 ml of diethyl ether. The combined ether extracts are evaporated to dryness and the residual yellow powder is extracted continuously with hot pentane for 3 h. Solvent removal yielded a yellow powder from which 0.40 g (19%) of large bright yellow crystals were obtained upon recrystallization from diethyl ether/pentane. M.p. 148–152°C, dec. ^{1}H NMR (200.13 MHz, $CDCl_3$): δ = 2.10 (s, 6H, CH_3C-3), 2.26 (d, 6H, CH_3C-2, $^3J_{PH}$ = 9.8 Hz), 6.41 (s, 5H, C_5H_5). ^{13}C NMR (50.32 MHz, $CDCl_3$): δ = 14.90 (s, CH_3C-3), 17.32 (d, CH_3C-2, $^2J_{PC}$ = 22.6 Hz), 115.93 (s, C_5H_5), 144.19 (d, C-3, $^2J_{PC}$ = 4.8 Hz), 148.59 (d, C-2, $^1J_{PC}$ = 51.4 Hz). ^{31}P NMR (80.00 MHz, $CDCl_3$): δ = 86.03. ^{91}Zr NMR

Table 4
Crystal data for compounds **3** and **4**

h3Compound	**3**		**4**
Formula	$C_{18}H_{26}Cl_2Zr$		$C_{13}H_{17}Cl_2PZr$
Mol. mass (g mol^{-1})	404.51		366.38
Crystal size (mm)	0.18 · 0.16 · 0.06		0.35 · 0.22 · 0.20
Temperature (K)	293(2)		173(2)
Diffractometer		CAD4	
Radiation; wavelength (Å)		Mo Kα; 0.71069	
Monochromator		graphite	
Scan-type, 2Θ-range	ω, 4.7-50°		$\omega - 2\Theta$, 4.3-60°
h; k; l-range	0,7; 0,20; 0,18		−12,0; −11,0; −28,28
Crystal system	Orthorhombic		Monoclinic
Space group	*Cmcm* (No. 63)		$P2_1/c$ (No. 14)
Unit cell dimensions:			
a (Å)	6.714(4)		8.8791(5)
b (Å)	17.275(4)		7.8051(8)
c (Å)	15.643(5)		20.9215(10)
β (°)	90		94.422(4)
V (Å^3)	1814(1)		1445.6(7)
Z	4		4
$D_{exp.}$ (g cm^{-3})	not determined		1.70
$D_{calcd.}$ (g cm^{-3})	1.481		1.683
F(000) (electrons)	832		736
μ (cm^{-1})	8.93		12.08
Absorption correction:	DIFABS [a]		7 Ψ-scans
max.; min.; av.	1.367; 0.717; 1.034		0.999; 0.915
Measured reflections	793		4757
Unique reflections	766 (R_{int} = 0.0198)		4189
Data for refinement (n)	760		3649 [$F_o^2 \geq 3\sigma(F_o^2)$]
Parameters refined (p)	80		154
$\Delta\rho$ [b]: max; min (e Å^{-3})	0.57; −0.36		0.68; −0.26
Programs [c]	SHELXS-86, SHELXL-93		MolEN
$R1$; $wR2$ [d] [I > 2σ(I)]	0.0488; 0.0911 [594]		
R; R_W [e]			0.0238; 0.0428
Goodness-of-fit, GOF	1.026 [f]		1.066 [g]
Weighting scheme, w	a; b [h]: 0.0494; 0.000		p [i]: 0.07

[a] Empirical absorption correction [67].
[b] Largest difference peak and hole.
[c] G.M. Sheldrick, SHELXL-93, Program for Crystal Structure Refinement, Göttingen 1993; SHELXL-86, Program for Crystal Structure Solution, Göttingen, 1986; MolEN, Molecular Structure Solution Procedures, Program Description, Delft Instruments, 1990.
[d] $R1 = (\Sigma \| F_o | - | F_c \|)/\Sigma | F_o |$; $wR2 = [\Sigma[w(F_o^2 - F_c^2)^2]/\Sigma[w(F_o^2)^2]]^{1/2}$.
[e] $R = (\Sigma \| F_o | - | F_c \|/\Sigma | F_o |$; $R_w = \Sigma w \| F_o | - | F_c \|^2/\Sigma w | F_o |^2]^{1/2}$.
[f] GOF = $[\Sigma[w(F_o^2 - F_c^2)^2]/(n-p)]^{1/2}$.
[g] GOF = $[\Sigma w \| F_o | - | F_c \|^2/(n-p)]^{1/2}$.
[h] $w = 1/[\sigma^2(F_o^2) + (aP)^2 + bP]$ where $P = (\max(F_o^2 \text{ or } 0) + 2F_c^2)/3$.
[i] $w = 1/[\sigma(F)]^2$, $\sigma(F) = \sigma(F^2)/2F$, $\sigma(F^2) = \{[\sigma(I)]^2 + [pF^2]^2\}^{1/2}$.

(37.33 MHz, CH_2Cl_2/CD_2Cl_2): $\delta = 29$ ($\omega_{1/2} = 1760$ Hz). MS (70 eV, 100°C): $m/e = 364$ (60%, $M^{+\cdot}$), 328 (100, $[M-HCl]^{+\cdot}$), 313 (22, $[M-HCl-CH_3]^+$), 299 (50, $[M-C_5H_5]^+$), 292 (41, $[M-2HCl]^+$), 271 (16, $[M-C_5H_5-C_2H_4]^+$), 259 (20, $[M-C_5H_5-HCl-2H_2]^+$)^2, 225 (47, $[M-C_4Me_4P]^+$), 199, (12, $[M-C_4Me_4P-C_2H_2]^+$), 190 (8, $[M-C_4Me_4P-Cl]^{+\cdot}$), 139 (19, $[C_4Me_4P]^+$), 123 (6, $[C_4Me_4P-CH_4]^+$). Anal. Found: C, 43.11; H, 4.49%. $C_{13}H_{17}Cl_2PZr$ (366.38); Calc.: C, 42.62; H, 4.68%.

4.6. $(C_4Me_4P)_2ZrCl_2$ (5) [21]

M.p. 120°C, dec. ^{91}Zr NMR (37.33 MHz, CH_2Cl_2/CD_2Cl_2): $\delta = 170$ ppm ($\omega_{1/2} = 3030$ Hz). MS (70 eV, 120°C): $m/e = 438$ (90%, $M^{+\cdot}$), 402 (36, $[M-HCl]^{+\cdot}$), 387 (11, $[M-HCl-CH_3]^+$), 299 (100, $[M-C_4Me_4P]^+$), 271 (22, $[M-C_4Me_4P-C_2H_4]^+$), 259 (23, $[M-C_4Me_4P-HCl-2H_2]^+$)^2, 139 (52, $[C_4Me_4P]^+$), 123 (6, $[C_4Me_4P-CH_4]^+$).

4.7. $(C_5Me_5)(C_5H_5)ZrCl_2$ (6) [55]

^{91}Zr NMR (37.33 MHz, CH_2Cl_2/CD_2Cl_2): $\delta = 10$ ppm ($\omega_{1/2} = 340$ Hz). MS (70 eV, 100°C): $m/e = 360$ (34%, $M^{+\cdot}$), 324 (100, $[M-HCl]^{+\cdot}$), 309 (10, $[M-HCl-CH_3]^+$), 295 (50, $[M-C_5H_5]^+$), 259 (20, $[M-C_5H_5-HCl]^+$), 255 (26, $[M-C_5H_5-HCl-2H_2]^+$)^2, 241 (5, $[M-C_5H_5-HCl-2H_2-CH_2]^+$), 225 (8, $[M-C_5Me_5]^+$), 199 (4, $[M-C_5Me_5-C_2H_2]^+$), 190 (6, $[M-C_5Me_5-Cl]^{+\cdot}$), 135 (14, $[C_5Me_5]^+$), 119 (30, $[C_5Me_5-CH_4]^+$), and further organic fragments.

4.8. $(C_5Me_5)_2ZrCl_2$ (7) [56]

^{91}Zr NMR (37.33 MHz, CH_2Cl_2/CD_2Cl_2): $\delta = 87$ ppm ($\omega_{1/2} = 140$ Hz). MS (70 eV, 160°C): $m/e = 430$ (54%, $M^{+\cdot}$), 394 (26, $[M-HCl]^{+\cdot}$), 379 (2, $[M-HCl-CH_3]^+$), 295 (100, $[M-C_5Me_5]^+$), 255 (20, $[M-C_5Me_5-HCl-2H_2]^+$)2, 241 (4, $[M-C_5Me_5-HCl-2H_2-CH_2]^+$), 136 (70, $[C_5Me_5H]^{+\cdot}$), 119 (24, $[C_5Me_5-CH_4]^+$), and further organic fragments.

4.9. Polymerizations

Polymerizations were carried out in a 1-l Büchi-glass autoclave, thermostatted to 70°C and charged with 300 ml toluene, MAO and the transition metal complex. The catalyst amount, concentration and Al : Zr ratio are specified in the respective Tables. After a preactivation time of 10 min the autoclave was pressurized with 5 bar ethylene and after 30 min the reaction was stopped by draining the toluene/polyethylene slurry into acidified water. The polymer was separated by filtration, washed with hexane and dried at 80°C. To ensure reproducibility polymerizations were carried out at least twice with each zirconium complex and a series of polymerization runs was performed with charges from the same toluene and MAO batch. To avoid ageing effects of MAO [57] a series of comparative polymerizations was run within a week.

4.10. Theoretical calculations

The semi-empirical ZINDO/1 geometry optimizations [58] were performed with the program HyperChem (Version 3.0, Autodesk Inc., Sausolito, CA 94965, USA).

The density-functional calculations [59] were carried out with the software package Unichem 2.3.1 containing the DF-program DGAUSS 2.3 from Cray Research Inc. A DZVP global orbital basis set together with an A1 global auxiliary basis set was used for the DF geometry optimizations with a Becke–Perdew nonlocal correction employed after final conversion.

For the potential energy calculations of the ring–Zr–ring bending mode the computations were performed within the extended-Hückel formalism [60] with weighted H_{ij}'s [61] and the use of the CACAO-program (Version 4.0) [62]. The atomic parameters for the elements involved in these EHMO calculations were as (H_{ii}, ζ): Zr 5s, −9.87 eV, 1.817; 5p, −6.76 eV, 1.776; 4d, −11.18 eV, 3.835, 1.505 (coefficients for double-ζ expansion: 0.6224, 0.5782) [63]; Cl 3s, −26.30 eV, 2.183; 3p, −14.20 eV, 1.733 [64]; P 3s, −18.6 eV, 1.60; 3p, −14.0 eV, 1.60 [65]; C 2s, −21.4 eV, 1.625; 2p, −11.4 eV, 1.625 [60]; H 1s, −13.6 eV, 1.3 [60]. Geometrical parameters were fixed as follows: Zr–C = 2.51, Zr–Cl = 2.44, $(C-C/P)_{Cp} = 1.42$, $C_{Cp}-H = 0.96$, $C_{Cp}-C_{Me} = 1.50$, $C_{Me}-H = 1.05$ Å, Cl–Zr–Cl = 98°.

4.11. X-Ray structure determinations of complexes 3 and 4

The crystals of **3** were grown by slow sublimation in vacuo, those of **4** from a diethyl ether/pentane solution upon cooling. In **3** all atomic positions including those

Table 5
Fractional atomic coordinates and equivalent isotropic displacement parameters (10^3 Å^2) for $(C_5Me_4H)_2ZrCl_2$, **3**

Atom	x	y	z	U_{eq} [a]
Zr	0.0621(2)	0.5000	0.2500	28(1)
Cl	−0.1768(3)	0.5000	0.3671(1)	50(1)
C1	0.3531(13)	0.4125(4)	0.2500	39(2)
C2	0.2435(9)	0.3918(3)	0.3233(3)	37(1)
C3	0.0636(10)	0.3560(3)	0.2957(3)	42(1)
C4	0.3121(14)	0.3987(4)	0.4146(4)	62(2)
C5	−0.0842(15)	0.3168(4)	0.3499(6)	76(2)

[a] U_{eq} is defined as one third of the trace of the orthogonalized U_{ij} tensor.

Table 6
Fractional atomic coordinates and equivalent isotropic thermal parameters (Å^2) for $(C_4Me_4P)(C_5H_5)ZrCl_2$, **4**

Atom	x	y	z	B_{eq} [a]
Zr	0.20817(2)	−0.16077(2)	−0.10749(1)	1.038(3)
Cl1	0.26848	0.10767(5)	−0.05007(2)	1.917(7)
Cl2	−0.04114(5)	−0.08060(7)	−0.15347(2)	2.201(8)
P	0.31842(6)	−0.34003(5)	−0.20498(2)	1.438(7)
C1	0.2519(2)	−0.1368(2)	−0.23130(8)	1.33(3)
C2	0.3336(2)	−0.0011(2)	−0.20059(7)	1.17(2)
C3	0.4540(2)	−0.0613(2)	−0.15699(8)	1.20(2)
C4	0.4587(2)	−0.2410(2)	−0.15216(8)	1.34(3)
C5	0.1287(2)	−0.1138(3)	−0.28404(9)	1.87(3)
C6	0.3040(2)	0.1857(2)	−0.21370(9)	1.57(3)
C7	0.5717(2)	0.0538(2)	−0.12450(9)	1.71(3)
C8	0.5844(2)	−0.3359(2)	−0.1144(1)	1.96(3)
C9	0.0413(2)	−0.3166(3)	−0.0340(1)	2.25(3)
C10	0.1560(3)	−0.2399(3)	0.00549(9)	2.12(3)
C11	0.2947(3)	−0.3146(2)	−0.00734(9)	1.92(3)
C12	0.2653(3)	−0.4426(2)	−0.05420(9)	1.93(3)
C13	0.1089(2)	−0.4415(2)	−0.07213(9)	2.07(3)

[a] B_{eq} is defined as $8/3\pi^2$ $[\Sigma_i\Sigma_j U_{ij} a_i^* a_j^* a_i a_j]$.

of the hydrogen atoms were found and refined (full-matrix least squares; nonhydrogen atoms with anisotropic temperature factors). In **4** the C-H positions are calculated with $d_{C\text{-}H} = 0.95$ Å and the isotropic temperature factors (B_{eq}) for these hydrogens were fixed to 1.3 B_{eq} of the parent carbon atom. Crystal data are listed in Table 4 [66]. Final positional parameters for nonhydrogen atoms are given in Tables 5 and 6 for **3** and **4**, respectively.

Acknowledgments

This work was supported by the Deutsche Forschungsgemeinschaft through grant Ja466/3-1, the Fonds der Chemischen Industrie and the Gesellschaft der Freunde der TU Berlin. We appreciate the continuous support by the Polyolefin Division of BASF AG, Ludwigshafen through the donation of chemicals, technical gases and the analyses of polymers. The TU Berlin is thanked for providing computer time and Dr. D.M. Proserpio (University of Milano) for a copy of the CACAO-program.

References and notes

[1] Examples for recent work: W. Kaminsky, *Angew. Makromol. Chem., 223* (1994) 101; F. Langhauser, J. Kerth, M. Kersting, P. Kölle, D. Lilge and P. Müller, *Angew. Makromol. Chem., 223* (1994) 155; C. Janiak and B. Rieger; *Angew. Makromol. Chem., 215* (1994) 47; M.L.H. Green and N. Ishihara, *J. Chem. Soc., Dalton Trans.*, (1994) 657; G. Erker and C. Mollenkopf, *J. Organomet. Chem., 283* (1994) 173; H.G. Alt, W. Milius and S.J. Palackel, *J. Organomet. Chem., 472* (1994) 113; W.-M. Tsai and J.C.W. Chien, *J. Polym. Sci., Part A: Polym. Chem., 32* (1994) 149; D. Fischer and R. Mülhaupt; *Makromol. Chem. Phys., 195* (1994) 1443; M. Bochmann, S.J. Lancaster, M.B. Hursthouse and K.M.A. Malik, *Organometallics, 13* (1994) 2235; G. Erker, C. Mollenkopf, M. Grehl, R. Fröhlich, C. Krüger, R. Noe and M. Riedel, *Organometallics, 13* (1994) 1950; Z. Guo, D.C. Swenson and R.F. Jordan, *Organometallics, 13* (1994) 1424; B. Rieger, G. Jany, R. Fawzi and M. Steimann, *Organometallics, 13* (1994) 647; G. Erker, M. Bendix and R. Petrenz; *Organometallics, 13* (1994) 456.

[2] B. Rieger and C. Janiak, *Angew. Makromol. Chem., 215* (1994) 35.

[3] P.C. Möhring and N.J. Coville; *J. Organomet. Chem., 479* (1994) 1.

[4] U. Stehling, J. Diebold, R. Kirsten, W. Röll, H.H. Brintzinger, S. Jüngling, R. Mülhaupt and F. Langhauser, *Organometallics, 13* (1994) 964.

[5] W. Spaleck, F. Küber, A. Winter, J. Rohrmann, B. Bachmann, M. Antberg, V. Dolle and E.F. Paulus, *Organometallics, 13* (1994) 954.

[6] W. Kaminsky, R. Engehausen, K. Zoumis, W. Spaleck and J. Rohrmann, *Makromol. Chem., 193* (1992) 1643.

[7] J. Tian and B. Huang, *Makromol. Rapid Commun., 15* (1994) 923.

[8] N. Piccolrovazzi, P. Pino, G. Consiglio, A. Sironi and M. Moret, *Organometallics, 9* (1990) 3098.

[9] I.-M. Lee, W.J. Gauthier J.M. Ball, B. Iyengar and S. Collins, *Organometallics, 11* (1992) 2115.

[10] P.C. Möhring and N.J. Coville, *J. Mol. Catal., 77* (1992) 41.

[11] P.C. Möhring, N. Vlachakis, N.E. Grimmer and N.J. Coville, *J. Organomet. Chem., 483* (1994) 159.

[12] J.A. Ewen, L. Haspeslagh, M.J. Elder, J.L. Atwood, H. Zhang and H.N. Cheng, in W. Kaminsky and H. Sinn (eds.), *Transition Metals and Organometallics as Catalysts for Olefin Polymerization*, Springer, Berlin, 1988, pp. 281–289.

[13] J.C.W. Chien and A. Razavi, *J. Polym. Sci., Part A: Polym. Chem., 26* (1988) 2369.

[14] T. Mise, S. Miya and H. Yamazaki, *Chem. Lett.*, (1989) 1853.

[15] D. Fischer, Ph.D. Thesis, University of Freiburg, Germany, 1992; D. Fischer and R. Mülhaupt, *J. Organomet. Chem., 417* (1991) C7.

[16] See, for example: G. Henrici-Olivé and S. Olivé, *Angew. Chem., 83* (1971) 121; *Ibid, Angew. Chem. Int. Ed. Engl., 10* (1971) 105. P. Diversi, L. Ermini, G. Ingrosso and A. Lucherini, *J. Organomet. Chem., 447* (1993) 291; F.J. Karol and S.-C. Kao, *New J. Chem., 18* (1994) 97.

[17] Examples for recent work: R.J. Meier, G.H.J. van Doremaele, S. Iarlori and F. Buda, *J. Am. Chem. Soc., 116* (1994) 7274. H. Weiss, M. Ehrig and R. Ahlrichs, *J. Am. Chem. Soc., 116* (1994) 4919; G. Guerra, L. Cavallo, G. Moscardi, M. Vacatello and P. Corradini, *J. Am. Chem. Soc., 116* (1994) 2988; E.P. Bierwagen, J.E. Bercaw and W.A. Goddard, III, *J. Am. Chem. Soc., 116* (1994) 1481; R. Gleiter, I. Hyla-Krispin, S. Niu and G. Erker, *Organometallics, 12* (1993) 3828; T.K. Woo, L. Fan and T. Ziegler, *Organometallics, 13* (1994) 2252; T. Yoshida, N. Koga and K. Morokuma, *Organometallics, 14* (1995) 746.

[18] C. Janiak, *J. Organomet. Chem., 452* (1993) 63; M.-H. Prosenc, C. Janiak and H.H. Brintzinger, *Organometallics, 11* (1992) 4036.

[19] H.J. R. de Boer and B.W. Royan, *J. Mol. Catal., 90* (1994) 171.

[20] R.D. Rogers, M.M. Benning, L.K. Kurihara, K.J. Moriarty and M.D. Rausch, *J. Organomet. Chem., 293* (1985) 51.

[21] F. Nief, F. Mathey, L. Ricard and F. Robert, *Organometallics, 7* (1988) 921.

[22] A.L. Spek, PLATON-93, PLUTON -92 graphics program, University of Utrecht, The Netherlands; A.L. Spek, *Acta Crystallogr., Sect. A, 46* (1990) C34.

[23] K. Prout, T.S. Cameron, R.A. Forder, S.R. Critchley, B. Denton and G.V. Rees, *Acta Crystallogr., Sect. B, 30* (1974) 2290.
[24] I.A. Ronova, N.V. Alekseev, N.I. Gapotchenko and Yu. T. Struchkov, *Zh. Strukt. Khim., 11* (1970) 584.
[25] T.N. Doman, T.K. Hollis and B. Bosnich, *J. Am. Chem. Soc., 117* (1995) 1352.
[26] U. Böhme, K.H. Thiele and A. Rufinska, *Z. Anorg. Allg. Chem., 620* (1994) 1455.
[27] P. Burger, K. Hortmann and H.H. Brintzinger, *Makromol. Chem., Macromol. Symp., 66* (1993) 127.
[28] P.G. Gassman, D.W. Macomber and J.W. Hershberger, *Organometallics, 2* (1983) 1470.
[29] P.G. Gassman and M.R. Callstrom, *J. Am. Chem. Soc., 109* (1987) 7875.
[30] R. Benn and A. Rufinska, *Angew. Chem., 98* (1986) 851; *Angew. Chem. Int. Ed. Engl., 25* (1986) 861.
[31] J.W. Lauher and R. Hoffmann, *J. Am. Chem. Soc., 98* (1976) 1729.
[32] C. Cauletti, J.C. Green, M.R. Kelly, P. Powell, J.V. Tilborg, J. Robbins and J. Smart, *J. Electr. Spectr. Rel. Phenom., 19* (1980) 327.
[33] S. Evans, M.L.H. Green, B. Jewitt, A.F. Orchard and C.F. Pygall, *J. Chem. Soc., Faraday Trans. II, 68* (1972) 1847.
[34] C. Guimon, D. Gonbeau, G. Pfister-Guillouzo, G. de Lauzon and F. Mathey, *Chem. Phys. Lett., 104* (1984) 560.
[35] P.M. Maitlis, *Chem. Soc. Rev., 10* (1981) 1.
[36] N.J. Coville, M.S. Loonat, D. White and L. Carlton, *Organometallics, 11* (1992) 1082.
[37] D. White and N.J. Coville, *Adv. Organomet. Chem., 36* (1994) 95.
[38] T. Uozumi and K. Soga, *Makromol. Chem., 193* (1992) 823.
[39] C. Janiak, K.C.H. Lange and P. Marquardt, *Macromol. Rapid Commun., 16* (1995) in press.
[40] G. Fink and W. Zoller, *Makromol. Chem., 182* (1981) 3265.
[41] K. Soga, H. Yanagihara and D. Lee, *Makromol. Chem., 190* (1989) 995.
[42] K.H. Reichert and K.R. Meyer, *Makromol. Chem., 169* (1973) 163.
[43] W. Kaminsky, K. Külper and S. Niedoba, *Makromol. Chem., Makromol. Symp., 3* (1986) 377.
[44] J.C.W. Chien and B.-P. Wang, *J. Polym. Sci. A: Polym. Chem., 26* (1988) 3089.
[45] W. Kaminsky, M. Miri, H. Sinn and R. Woldt, *Makromol. Chem. Rapid Commun., 4* (1983) 417.
[46] J.A. Ewen, *J. Am. Chem. Soc., 106* (1984) 6355.
[47] C. Janiak, B. Rieger, R. Voelkel and H.G. Braun, *J. Polym. Sci. A: Polym. Chem., 31* (1993) 2959, and references therein.
[48] L.A. Nekhaeva, G.N. Bondarenko, S.V. Rykov, A.I. Nekhaev, B.A. Krentsel, V.P. Mar'in, L.I. Vyshinskaya, I.M. Khrapova, A.V. Polonskii and N.N. Korneev, *J. Organomet. Chem., 406* (1991) 139.
[49] J. Tian and B. Huang, *Macromol. Rapid Commun., 15* (1994) 923.
[50] C. Janiak and K.C.H. Lange, unpublished results.
[51] J.C.W. Chien and B.-P. Wang, *J. Polym. Sci. A: Polym. Chem., 27* (1989) 1539.
[52] J.C.W. Chien and B.-P. Wang, *J. Polym. Sci. A: Polym. Chem., 28* (1990) 15.
[53] E.C. Lund and T. Livinghouse, *Organometallics, 9* (1990) 2426.
[54] P. Courtot, R. Pichon, J.Y. Salaun and L. Toupet, *Can. J. Chem., 69* (1991) 661.
[55] P.T. Wolczanski and J.E. Bercaw, *Organometallics, 1* (1982) 793.
[56] J.M. Manriquez, D.R. McAlister, E. Rosenberg, A.M. Shiller, K.L. Williamson, S.I. Chan and J.E. Bercaw, *J. Am. Chem. Soc., 100* (1978) 3078.
[57] S. Lasserre and J. Derouault, *Nouv. J. Chim., 7* (1983) 659.
[58] A.D. Bacon and M.C. Zerner, *Theor. Chim. Acta, 53* (1979) 21; M.C. Zerner, G.H. Loew, R.F. Kirchner and U.T. Mueller-Westerhoff, *J. Am. Chem. Soc., 102* (1980) 589; M.C. Zerner, in K.B. Lipkowitz and D.B. Boyd (eds.), *Reviews in Computational Chemistry*, Vol. II, VCH Weinheim, 1991, pp. 313–365.
[59] T. Ziegler, *Chem. Rev., 91* (1991) 651.
[60] R. Hoffmann, *J. Chem. Phys., 39* (1963) 1397; R. Hoffmann and W.N. Lipscomb, *J. Chem. Phys., 36* (1962) 2179; R. Hoffmann and W.N. Lipscomb, *J. Chem. Phys., 37* (1962) 2872.
[61] J.H. Ammeter, H.-B. Bürgi, J.C. Thibeault and R. Hoffmann, *J. Am. Chem. Soc., 100* (1978) 3686.
[62] C. Mealli and D.M. Proserpio, *J. Chem. Ed., 67* (1990) 399.
[63] K. Tatsumi, A. Nakamura, P. Hofmann, P. Stauffert and R. Hoffmann, *J. Am. Chem. Soc., 107* (1985) 4440.
[64] R.H. Summerville and R. Hoffmann, *J. Am. Chem. Soc., 98* (1976) 7240.
[65] S. Shaik, R. Hoffmann, C.R. Fisel and R.H. Summerville, *J. Am. Chem. Soc., 102* (1980) 4555. C.N. Wilker and R. Hoffmann, *J. Am. Chem. Soc., 105* (1983) 5285.
[66] Further details of the crystal structure determinations are available on request from the Fachinformationszentrum Karlsruhe, Gesellschaft für wissenschaftlich-technische Information mbH, D-76344 Eggenstein-Leopoldshafen on quoting the depository number CSD-401735 for **3** and CSD-40177 for **4**, the authors, and the journal citation.
[67] N.G. Walker and D. Stuart, *Acta Crystallogr., Sect. A, 39* (1983) 158.